



Published in final edited form as:

Nat Commun. ; 5: 5762. doi:10.1038/ncomms6762.

THE CDC13-STN1-TEN1 COMPLEX STIMULATES POL α ACTIVITY BY PROMOTING RNA PRIMING AND PRIMASE-TO-POLYMERASE SWITCH

Neal F. Lue¹, Jamie Chan¹, Woodring E. Wright², and Jerard Hurwitz³

¹Department of Microbiology & Immunology, W. R. Hearst Microbiology Research Center, Weill Medical College of Cornell University, New York, New York, 10065

²Department of Cell Biology, University of Texas Southwestern Medical Center, Dallas, Texas, 75390

³Molecular Biology Program, Memorial Sloan-Kettering Cancer Center, New York, New York, 10065

Abstract

Emerging evidence suggests that Cdc13-Stn1-Ten1 (CST), an RPA-like ssDNA-binding complex, may regulate primase-Pol α (PP) activity at telomeres constitutively, and at other genomic locations under conditions of replication stress. Here we examine the mechanisms of PP stimulation by CST using purified complexes derived from *Candida glabrata*. While CST does not enhance isolated DNA polymerase activity, it substantially augments both primase activity and primase-to-polymerase switching. CST also simultaneously shortens the RNA and lengthens the DNA in the chimeric products. Stn1, the most conserved subunit of CST, is alone capable of PP stimulation. Both the N-terminal OB fold and the C-terminal winged-helix domains of Stn1 can bind to the Pol12 subunit of the PP complex, and stimulate PP activity. Our findings provide mechanistic insights on a well-conserved pathway of PP regulation that is critical for genome stability.

Pol α , one of the three major replicative DNA polymerases in eukaryotes^{1,2}, is distinguished from the other replicative polymerases in having a tightly associated primase activity³. The primase-Pol α (PP) complex consists of four subunits: Pol1, the DNA polymerase; Pol12, a “scaffold” subunit that mediates interactions with regulatory factors^{4,5}; Pri1, the primase catalytic subunit; and Pri2, the large and non-catalytic primase subunit^{6,7}. In chromosomal DNA replication, PP performs the task of the true initiator: it synthesizes a short RNA

Users may view, print, copy, and download text and data-mine the content in such documents, for the purposes of academic research, subject always to the full Conditions of use:http://www.nature.com/authors/editorial_policies/license.html#terms

Correspondence to: Neal F. Lue.

Contact: Neal F. Lue, nflue@med.cornell.edu.

Author Contributions

N.F.L. designed and performed most of the experiments with assistance from J.C. W.E.W and J.H. contributed reagents. N.F.L. analyzed the data and wrote the manuscript incorporating comments from J.H.

Competing Financial Interests Statement

The authors report no competing financial interests.

primer of ~7–10 nt and extends it by an additional 10–20 dNMP before dissociating from the template/product duplex^{8,9}. The 3' terminus of the RNA-DNA chimera then serves as the primer for DNA synthesis by DNA polymerase ϵ and δ on the leading and lagging strands, respectively¹⁰. Though the DNA polymerase activity of Pol α can be assayed using synthetic template/primer substrates, prevailing evidence suggests a tight “communication” between the primase and Pol α such that the latter preferentially extends RNA primers synthesized by the former subunit⁹.

Telomeres, the special nucleoprotein structures located at the ends of linear eukaryotic chromosomes, are critical for chromosome stability; they protect the DNA termini from degradation, end-to-end fusion, and other abnormal transactions^{11–13}. Owing to the incomplete end replication problem¹⁴, the maintenance of telomere DNA requires not only efficient semi-conservative DNA replication, but also terminal repeat addition. In most organisms, telomeric DNA consists of short repeats that are rich in G and C residues on the 3' and 5'-end bearing strands, respectively. These two complementary strands of telomeres, designated the G- and C-strands, are “extended” sequentially by the telomerase and the PP complex; telomerase lengthens the G-strand through reverse transcription of an integral RNA template subunit^{15–17}, whereas PP lengthens the C-strand by copying the extended G-tail^{18–20}. The initial RNA-DNA chimera is presumably processed and ligated to the original 5' end to yield the mature C-strand. Thus, the extension of telomeres is a multi-step process that entails the action of multiple enzymes, including PP. Because semi-conservative replication through telomeres also requires PP, this complex evidently participates in multiple telomere maintenance pathways, and may thus be subjected to elaborate regulation at chromosome ends.

Compelling evidence for special regulation of PP at telomeres came from analysis of the Cdc13-Stn1-Ten1 (CST) complex, a conserved G strand-binding complex^{21–23}. Initially discovered in the budding yeast *Saccharomyces cerevisiae* (*Sc*), the CST complex mediates critical functions in both telomere protection and maintenance. Mutations in subunits of the complex are often lethal, and hypomorphic alleles of CST genes were found to engender a wide variety of aberrations including telomere length alterations, telomere degradation, and excessive recombination. Consistent with a role in telomere protection, the phenotypes of some CST mutants can be suppressed by checkpoint and nuclease mutations^{24,25}. In support of the telomere maintenance function, CST is known to associate with both telomerase and PP subunits, and is proposed to regulate the activity of both enzymes. Notably, the recent discovery and characterization of CST complexes in vertebrates suggest that PP regulation may be an especially well-conserved function of this complex^{26–28}. In particular, the two largest subunits of the vertebrate complex (CTC1 (equivalent to fungal Cdc13) and STN1) were initially purified and analyzed as Pol α -associated stimulatory factors (AAF-132 and AAF-44)^{29,30}. Moreover, genetic depletion or disruption of vertebrate CST subunits does not cause immediate and generalized telomere de-capping, suggesting that the vertebrate complex plays a minor role in telomere protection^{31–33}. Instead, loss of human or mouse CST subunits caused defects in telomere replication and C-strand fill-in synthesis, which are better explained by a function of CST in PP regulation at telomeres^{31–35}. Depletion of vertebrate CST also impaired cellular recovery from replication stress, suggesting a non-

telomeric function. Besides its multiplicity of functions, CST is notable for its resemblance to RPA, the major ssDNA-binding complex in eukaryotes^{36,37}. RPA, which mediates diverse functions in replication, recombination, and repair, is also composed of three subunits (Rpa1, Rpa2, and Rpa3)³⁸, and the two smaller subunits of the CST and RPA complexes manifest unmistakable structural and functional similarities^{36,37,39}. Nevertheless, CST and RPA are clearly not redundant, and the distinctions between the two complexes are major topics of ongoing investigations.

Notwithstanding the wealth of molecular genetic data on the role of CST in promoting DNA synthesis at telomeres and elsewhere, the biochemical mechanisms that undergird this regulation remain poorly understood. The physical basis for CST-PP interaction has not been elucidated. The precise molecular step(s) of the PP reaction cycle enhanced by the CST complex remains a subject of debate, with models favoring template-binding, priming, and DNA polymerization all having been proposed^{29,30,40}. Also unclear is the extent of evolutionary conservation between the vertebrate and fungal CST in regards to PP regulation. Studies of fungal CST mechanisms have been hampered by difficulties in isolating adequate quantities of the complex for detailed biochemical investigations. We recently overcame this obstacle by obtaining high levels of CST from *Candida glabrata*⁴¹, a pathogenic fungus that is evolutionarily close to *S. cerevisiae*. In this report, we explore the regulation of *C. glabrata* PP complex by CST, and show for the first time that the primase-Pol α stimulatory activity of CST is conserved in fungi. By characterizing the effect of CST on individual steps of the PP reaction cycle, we deduce that while CST has no effect on the isolated DNA polymerase activity, it can substantially enhance the priming reaction and the primase-to-polymerase switch. We also home in on Stn1 as the CST subunit responsible for PP stimulation, and show that this subunit makes multiple, functionally important contacts with the Pol12 subunit. Finally, we demonstrate that this pathway of PP regulation is extremely well conserved in evolution. Our findings establish a biochemical framework for interpreting the physiologic effects of CST.

RESULTS

The PP complex catalyzes the synthesis of RNA-DNA chimeras

To investigate the regulation of PP by CST *in vitro*, we first isolated the two complexes encoded by *C. glabrata*. CST was obtained through recombinant co-expression and affinity purification from *E. coli* (Supplementary Fig. 1a)⁴¹, whereas PP through tagging of the Pri2 subunit and affinity purification from *C. glabrata* (Supplementary Fig. 1b). The PP complex can be further purified to near homogeneity by glycerol gradient fractionation (Supplementary Fig. 1c). The affinity-purified and glycerol gradient-purified PP behaved identically in all the polymerization assays used in the current study (Supplementary Fig. 1d). Before analyzing the effect of CST, we characterized the synthesis of RNA-DNA chimeras by PP alone on poly-dT and two model G-tail substrates (Fig. 1a and Supplementary Table 1). Physiologic concentrations of ribonucleotides and deoxyribonucleotides (including P³²-dATP) were used in the assays to mimic the *in vivo* condition⁴². Because the synthesis of detectable products required the action of both primase and DNA polymerase, this assay will be referred to as the coupled primase-polymerase

assay. Labeled products that ranged in size from about 10 nt to 40 nt were generated in these reactions. The product size distribution was quite narrow for the poly-dT template, manifesting a sharp peak at ~20–25 nt. In comparison, the C-strand products were more heterogeneous in size such that short (10–20 nt) and long (30–40 nt) products were as well represented as the medium-sized products (Fig. 1a). As predicted for PP-mediated synthesis of C-strand RNA-DNA chimeras, product accumulation required the presence both ribonucleotides and deoxyribonucleotides (Fig. 1b). Also consistent with the composition of the *C. glabrata* C-strand, omitting rCTP had more a detrimental effect than omitting other ribonucleotides on product synthesis. The different size distribution of the poly-dT and G-tail products indicates that the polymerization property of PP is sequence-dependent, as noted in a recent study⁴³.

CST stimulates PP and alters the lengths of RNA and DNA

Having detected PP activity on ssDNA templates, we next determined the effect of purified recombinant CST using this assay. In the standard coupled assay, CST stimulated the synthesis of RNA-DNA chimeras on poly-dT by ~5 fold and on the G-tail by ~2–3 fold (Fig. 1c). Owing to the greater magnitude of stimulation, the detailed mechanism of PP stimulation by CST was characterized using primarily the poly-dT template. However, stimulation of PP activity on G-tail templates was also reproducibly observed, especially at low PP concentrations. Time course analysis indicates that for the poly-dT template, the enhanced product accumulation in the presence of CST was due to an increase in the rate of synthesis (Supplementary Fig. 2a). The magnitude of stimulation was CST concentration-dependent, reaching a maximum at ~100–150 nM (Supplementary Fig. 2b). The degree of stimulation was also affected by PP concentration, being highest at low to moderate levels of the polymerase in the presence of a fixed CST concentration (Supplementary Fig. 2c, d). Notably, these findings are consistent with early analyses of mammalian AAF^{29,30}, suggesting that despite the low level of sequence identity between the fungal and mammalian CST complexes (especially in regard to CTC1/Cdc13 and Ten1), the mechanism of PP regulation appears similar.

CST not only stimulated product synthesis, but also caused a small but reproducible shift in the length distribution of the products; the center of the product peak was longer by ~0.5–1.0 nt in the presence of CST compared with that found in its absence (Fig. 1d, lane 1 and 2; Supplementary Fig. 3a). This alteration could be due to a change in the RNA or DNA length (or both) in the chimera. To distinguish between these possibilities, we subjected the products to alkaline hydrolysis, which completely removed the RNA portions from the chimeras. Remarkably, the center of the “DNA only” product peak was longer by ~1.5 to 2 nt when CST was included in the PP reaction (Fig. 1d, lane 3 and 4; Supplementary Fig. 3a), implying that CST simultaneously shortened the RNA and lengthened the DNA synthesized by PP. We then used an alternative method to assess the lengths of the RNA primer, i.e., by subjecting the chimeric products to DNase I treatment. This nuclease is known to cleave within the DNA portion of the chimera, leaving ~2–3 nt of labeled DNA attached to the RNA⁸. Interestingly, the most abundant cleavage product derived from the CST-plus reaction is ~1 nt shorter than that from the CST-minus reaction, again supporting the idea

that CST shortened the RNA primer (Supplementary Fig. 3b). Our finding points to unexpectedly complex effects of CST on PP-mediated product synthesis.

To assess the generality of the CST effects, we compared the distribution of products on G-tail templates. However, the heterogeneous nature of the C-strand products from the *C. glabrata* G-tail (CgG4) complicated the interpretation of results. We tested several alternative templates, and found that one consisting of 9 copies of the human G-strand repeat (HsG9) yielded regular and interpretable results (Supplementary Fig. 3c). On this template, several clusters of products that are ~6 nt apart can be detected in the absence of CST, presumably due to preferential initiation and termination of product synthesis at specific nucleotides within the repeat unit. Interestingly, the center of the product peak within each cluster was also increased by about one nucleotide in the presence of CST. Hence, the effect of CST on PP product lengths can be observed on both non-telomeric and telomeric templates.

CST stimulates RNA priming and primase-to-polymerase switch

A priori, the stimulatory effect of CST on total product synthesis can be due to an enhancement of the primase or DNA polymerase reaction, or the “coupling” between the two active sites. To distinguish between these possibilities, we first analyzed the effect of CST in separate primase and DNA polymerase reactions. For the primase-only assay, PP was incubated with poly-dT in the presence of labeled ATP as the sole nucleotide. Previous studies indicate that eukaryotic primase preferentially synthesizes unit-length primers (7–10 nt) or multiples thereof (i.e., multiples of 7–10 nt) in the absence of dNTP. Indeed, we observed both unit-length primers and dimers in our assays (Fig. 2a). More interestingly, the effect of CST in this assay was ATP concentration-dependent: CST stimulated primer synthesis by 2–3 fold in 20 μ M ATP, but had much less effect in 400 μ M ATP (Fig. 2a). As a complementary test, we performed a standard primase assay, which combines primer synthesis (using unlabeled 3 mM ATP) with extension by Klenow (using labeled dATP)². Because Klenow was included in excess, the dATP incorporation was proportional to the RNA primers produced in the reaction. Using this assay, we found little stimulation of primase activity by CST (Fig. 2b). Thus, CST preferentially enhances primase activity at low ATP concentrations. We then performed polymerase-only assays, for which we used “pre-primed” Poly-dT/rA₁₀ template and dATP as the substrate (Fig. 2c). No enhancement of DNA synthesis was observed in the presence of CST, indicating that the complex does not stimulate the DNA polymerase activity. We reasoned that the DNA template/RNA primer generated by primase might behave differently from the synthetic Poly-dT/rA₁₀ substrate, and hence performed an alternative assay. In this assay, we first allowed PP to synthesize unlabeled oligo-rA using ATP as the sole nucleotide substrate. Upon completion of RNA synthesis, free ATP was removed from the reaction, and the resulting Poly-dT/oligo-rA mixture used as the substrate for DNA synthesis by PP in the absence or presence of CST (Fig. 2d). CST again had no effect on DNA synthesis, indicating that it does not stimulate “isolated” DNA polymerase α activity.

We then directly analyzed the efficiency of primase-to polymerase switch using labeled ATP and unlabeled dATP in the coupled assay. Strikingly, at both 20 and 400 μ M ATP,

CST increased the switch efficiency; the levels of unit-length primers were substantially reduced, and the levels of RNA-DNA chimeras elevated (Fig. 2e). The characteristic increase in the length of the chimeric products was also observed. By quantifying the levels of RNA and RNA-DNA chimeras, we infer that CST reduced the termination frequency (i.e., the fraction of 7, 8, 9, and 10-mer RNAs that were not lengthened to form RNA-DNA chimeras) from ~0.25 to ~0.05 (Fig. 2f). These findings provide direct support for the notion that CST stimulates DNA synthesis by raising the efficiency of the primase-to-polymerase switch. In addition, by quantifying the total number of RNA and RNA-DNA oligomers, we showed that CST stimulated RNA priming by ~2 fold at 20 μ M ATP, and by ~50% at 400 μ M ATP (Fig. 2g). Thus, the overall increase in the level of RNA-DNA chimeras in the presence of CST is due to the combined effect of CST on the primase activity and the primase-to-polymerase switch.

To examine further the mechanisms of stimulation, we performed a set of primer capping assays, which are identical to switch assays except that dATP is replaced by ddATP (Supp. Fig. 4)⁴⁴. The capping assay allows RNA priming and switch to take place, but limits the extension of oligo-rA to a single deoxynucleotide. Because the oligo-rA-ddA products exhibit characteristic differences in mobility from the oligo-rA products, it is possible to assign the identity of the oligomers with high confidence, and thereby characterize the reactions in greater detail (Supp. Fig. 4a). By comparing the product distributions in the unit-size primer range, we can clearly detect evidence for the stimulation of priming by CST in 20 μ M ATP (compare trace 1 and 2, and 3 and 4 in Supp. Fig. 4b), and for stimulation of switch by CST in 400 μ M ATP (compare trace 7 and 8 in Supp. Fig. 4b). Altogether, our collection of assays revealed multiple effects of the CST complex on different steps of nucleic acid synthesis by PP.

The Stn1 subunit of CST is responsible for PP stimulation

To determine the subunit(s) of the CST complex responsible for PP stimulation, we prepared and tested isolated subunits. Each subunit was expressed in *E. coli*, purified by affinity chromatography (Supplementary Fig. 1a), and found to be free of contaminating polymerase activity. Notably, neither Cdc13 nor Ten1 was capable of stimulating PP. Because we had previously shown that recombinant Cdc13 alone is active in DNA binding, its inability to stimulate PP cannot be attributed to gross misfolding⁴¹. In contrast to Cdc13 and Ten1, Stn1 alone was nearly active as the intact CST complex in PP stimulation (Fig. 3a). The effect of Stn1 can be observed on both the Poly-dT and *C. glabrata* G-tail templates (Fig. 3a, left and right panels). Stn1 contains an N-terminal OB fold domain that is implicated in DNA binding, and a C-terminal duplicated winged-helix domain that is proposed to contact other proteins^{36,37,39,41}. We purified these two domains separately (Supplementary Fig. 1a) and found that each was competent in PP stimulation (Fig. 3b). All the Stn1 variants (i.e., full length, N-terminus and C-terminus) caused the characteristic lengthening of products described earlier for the intact CST complex, suggesting that their mechanisms of stimulation are likely to be similar. Titration of CST and Stn1 variants in the Poly-dT assays indicates that CST, Stn1, and Stn1N have comparable activities, while Stn1C is somewhat less active in PP stimulation (Fig. 3c, d). Thus, the PP-regulatory function of CST appears to

reside largely in the Stn1 subunit, which possesses at least two determinants for promoting PP activity.

Stn1 makes multiple contacts with Pol12

The complex effect of CST and Stn1 on PP products suggests allosteric control that could be mediated by protein-protein interactions between subunits of the two complexes. The putative interaction between CST and PP was confirmed using a GST pull down assay. Purified CST complex was immobilized on glutathione-Sepharose through the GST tag on Ten1. Whole cell extracts from the *C. glabrata* strain carrying FLAG₃-tagged Pri2 were incubated with the CST-containing beads, and CST-associated proteins in pull down samples analyzed for polymerase activity as well as Pri2-FLAG₃ protein. As predicted, the CST pull down samples contained higher levels of polymerase activity as well as Pri2-FLAG₃, indicating that the two complexes can physically associate with each other (Supplementary Fig. 5).

Previous analysis points to two possible contacts between CST and PP: one between Cdc13 and Pol1 and the other between Stn1 and Pol12^{19,45,46}. That Stn1 alone but not Cdc13 is able to stimulate PP suggests that the latter interaction may be functionally more important. We therefore examined the physical interaction between Stn1 and Pol12 using a co-expression/affinity purification assay. The two proteins were expressed separately or together in *E. coli* as His₆-SUMO and GST-FLAG fusion proteins, respectively. Extracts were prepared and subjected to affinity purification to assess complex formation. As hypothesized, His₆-SUMO-Stn1 and GST-FLAG-Pol12 remained stably associated with each other following both Ni-NTA and anti-FLAG affinity chromatography (Fig. 4a). Moreover, the two polypeptides are present at a 1:1 ratio, suggesting a 1:1 stoichiometry. Surprisingly, when Stn1 and Pol12 were first separately purified, and then subjected to anti-FLAG or Glutathione pull down assays, little interaction was detected between the two proteins. This observation suggested that one of the proteins may adopt an unproductive conformation when it is expressed in the absence of the other. Because Stn1 alone is active in PP stimulation, we suspect that isolated Pol12 may adopt an aberrant conformation. Indeed, an existing crystal structure of the *Sc*Pol1-Pol12 complex revealed extensive contacts between Pol12 and the C-terminus of Pol1⁴⁷, suggesting that Pol1 may influence Pol12 conformation. We then tested the N- and C-terminal domains of Stn1 and found that each domain can independently bind Pol12 (Fig. 4b). Thus, the ability of both the N- and C-terminus of Stn1 to stimulate PP activity correlates with their binding to Pol12.

To characterize the functional significance of Stn1-Pol12 interaction, we further dissected the C-terminal winged-helix domain of Stn1, which contains two winged-helix repeats, named WH1 and WH2. Each repeat was expressed and purified as a His₆-SUMO fusion protein, and then tested for PP stimulatory activity on the poly-dT template. Only WH2 showed significant stimulatory activity, implying that this repeat is responsible for the stimulatory function of Stn1C (Fig. 3e). Indeed, only WH2 showed detectable binding to Pol12 in the co-expression/pull down assay, suggesting that the physical interaction is necessary for Stn1-mediated PP stimulation (Fig. 4c). We also attempted to identify point mutations in Stn1C that disrupt the Stn1-Pol12 interaction. The mutations examined are

clustered near the central β -sheet of the winged-helix repeats, which is thought to be the main protein-binding surface in this motif⁴⁸. Several of the alleles correspond to *S. cerevisiae* alleles that were previously shown to cause telomere lengthening³⁶. Altogether, we generated and analyzed five Stn1C mutant alleles, two in the first and three in the second winged-helix repeat (Supplementary Table 2, Supplementary Fig. 6a). Interestingly, none of the substitution mutant lost its association with Pol12, even though most mutant alleles were expressed at lower levels than wild type Stn1C, possibly due to structural perturbations (Supplementary Fig. 6b). Consistent with the binding results, all of the point mutants retained stimulatory function in PP activity assays (Supplementary Fig. 6c). Thus, The WH2 motif of Stn1C may use a novel, non- β strand surface to mediate Pol12 binding and PP stimulation. In addition, the telomere lengthening effect of comparable ScSTN1 mutations was probably not due to altered binding to Pol12.

Conservation of PP regulation by Stn1 in fungi and humans

Even though mammalian CST is known to bind and stimulate mammalian PP, the mechanistic basis of this regulation is largely undefined. To determine if the mechanisms we defined in fungi are applicable to other organisms, we examined the activities of purified human PP (*HsPP*) and human STN1 (*HsSTN1*) using the same assays. In the standard coupled assays on the poly-dT template, *HsPP* generated chimeric products that are slightly longer than those of *CgPP*, but otherwise displayed similar properties with respect to template and nucleotide utilization (Fig. 5a, lane 1 and 4). In general agreement with the fungal studies, *hsSTN1* alone stimulated product synthesis by *hsPP* and increased the lengths of the RNA-DNA chimera slightly (Fig. 5a, lane 1 and 2). Likewise, in the primase-to-polymerase switch assays, *hsSTN1* increased the total number of RNA and RNA-DNA oligomers (by ~70%), and reduced the fraction of the RNA primers that terminated at the priming stage (by ~30%) (Fig. 5b). (Note that while the levels of un-extended RNA oligomers were similar in lane 1, 2 and 3, the higher levels of total reaction products in lane 2 and 3 indicate that the fractions of un-extended RNA primers were lower for these two reactions.) Remarkably, despite the very low level of sequence similarity between *CgStn1* and Human STN1 (*HsSTN1*) (~17% identity and 33% similarity), both proteins displayed substantial stimulatory activities on the heterologous PP complex (Fig. 5a). In a side-by-side comparison of the two proteins in Poly-dT assays over a range of concentrations, *HsSTN1* is only about 2-fold less active than *CgStn1* in stimulating *CgPP* (Supplementary Fig. 6d).

The “cross-species” stimulation of PP by Stn1 suggests that the protein interface between Pol12 and Stn1 may be quite similar in humans and *C. glabrata*. To test this possibility, we examined all the potential pair-wise interactions between the Pol12 and Stn1 orthologues from *C. glabrata* and humans using the co-expression/affinity purification assay described in the previous section. Consistent with a high degree of conservation of the Stn1-Pol12 interface, we observed co-purification between all the intra-species and inter-species protein pairs on Glutathione-Sepharose (Fig. 5c). We surmise that the relevant features of the Stn1-Pol12 interaction have been preserved between fungi and mammals notwithstanding one billion years of evolution.

DISCUSSION

The chief significance of the current report resides in the demonstrations that the fungal CST complex stimulates PP activity *in vitro*, that this regulation is due to an enhancement of both RNA priming and the primase-to-polymerase switch, that Stn1-Pol12 interaction provides the physical basis for this regulation, and that this regulatory mechanism is well conserved in evolution. The implications for these findings are discussed below.

Seminal studies on the priming and switch reactions, as well as recent structural analysis of the holoenzyme offer a framework for interpreting the current results^{8,9,44}. The early experiments indicate that (i) only primers of sufficient lengths (7 nucleotides or longer) can be utilized by the DNA polymerase, (ii) the efficiency of the primase-to-polymerase switch is highly dependent on temperature, template concentration, and deoxynucleotide concentration. In general, conditions that favor the stability and formation of RNA-DNA hybrid (e.g., low temperature and high template concentration) or DNA synthesis (e.g., high deoxynucleotide concentration) appear to enhance the switch efficiency⁸. The recent structural analysis of the architecture of the primase-Pol α complex provides additional clues to the “switch” process. Based on cryo-electron microscopy image reconstruction, the holoenzyme adopts a dumbbell configuration with two mobile lobes⁴⁴. One lobe is occupied by the catalytic domain of Pol1, and the other by Pol12, Pri1, Pri2, and the C-terminal domain (CTD) of Pol1, respectively. This model suggests plausible means by which Stn1 regulates priming and the switch reaction. For example, Pol12, upon binding Stn1, is well positioned to regulate primase activity because of their close physical proximity. In addition, the large distance between the centers of the two PP lobes (the presumed active sites of the enzymes) implies that a coordinated conformational change may be required for the handoff reaction⁴⁴. One possible consequence of Stn1-Pol12 interaction may hence be a conformational change in PP that brings the two lobes closer together to enhance the coordination between the active sites. More efficient transfer of the DNA-RNA hybrid from the primase to polymerase active site may also enable a greater fraction of short RNA primers (which are less efficient substrate for the DNA polymerase) to be extended into chimeric products, resulting in a shortening of the average length of the RNA in the chimera. Structural and single-molecule analyses will likely be necessary to achieve understanding of the physical basis of the complex regulatory effects of CST on PP.

The modulation of the primase-to-polymerase switch represents an unprecedented means for regulating PP activity. Our finding raises the possibility that other factors may regulate PP in a similar fashion. In particular, the paralogous RPA complex has been reported to stimulate the DNA polymerase activity and processivity of Pol α ⁴⁹. However, the stimulatory activity of RPA was attributed to Rpa1 rather than the Stn1 paralog Rpa2. Because the substrates and assays used in the RPA study are different from those in the current report, the potential role of Rpa2 in PP stimulation warrants further investigation. In this regard, we note that Rpa2 also possesses an N-terminal OB fold and a C-terminal winged-helix domain (albeit just one iteration of the winged-helix motif).

The discovery of the PP stimulatory activity of the *C. glabrata* CST complex adds to the growing evidence for functional conservation between vertebrate and fungal CST,

previously thought to be limited because of poor sequence conservations between subunits of the complexes, and the very different routes of discovery. As noted before, while the fungal CST complex was initially characterized as a telomere-capping complex, the vertebrate factors were initially purified owing to their Pol α stimulatory activity. Even though studies to date have not revealed a direct telomere-protective function for vertebrate CST, the current report leaves little doubt that the fungal complex stimulates PP. Thus PP regulation appears to be a more ancient and conserved function of CST, whereas telomere capping a more recent and specific acquisition of the fungal complex. Moreover, the mechanisms of PP enhancement appear to be similar if not identical between the fungal and vertebrate complexes, as evidenced by the ability of both *HsSTN1* and *CgStn1* to stimulate the primase-to-polymerase switch. Indeed, the ability of fungal and human *Stn1* to bind heterologous Pol12 and stimulate heterologous PP indicates that the *Stn1*-Pol12 interface has been retained through 1 billion years of evolution.

The regulatory mechanism we uncovered is likely to extend to non-fungal and non-vertebrate organisms because most *Stn1*s in these organisms also contain an N-terminal OB fold and a C-terminal duplicated winged-helix domain. Thus, they have the potential of making multiple contacts to Pol12 to stimulate PP. An interesting case is presented by the plant *Stn1* orthologues, which are unusually small and lack the C-terminal winged-helix domain⁵⁰. Nevertheless, because the OB fold domain of *CgStn1* alone exhibits a PP stimulatory activity, this function could very well be conserved in the plant homologues as well.

Two intriguing notions concerning the regulation of DNA replication *in vivo* can be proposed based on previous findings and the current observations. The first relates to the control of dormant origins. As noted before, CST is implicated in replication at telomeres constitutively and elsewhere under conditions of replication stress^{31–35}. Interestingly, at least in the context of HU-mediated replication stress, CST appears to promote the firing of dormant origins, but not fork restart³². Our data suggest that CST may regulate PP both at the priming and the primase-to-polymerase switch steps, implying that these could be the rate limiting steps for dormant origin firing *in vivo*. The second notion concerns the role of CST and Pol α in checkpoint regulation. Pol α has long been known to play a role in S-phase checkpoint activation, but the underlying mechanisms are poorly understood^{51–53}. A recent report demonstrates that overexpression of *Stn1C* in *S. cerevisiae* renders the cells highly sensitive to HU by blocking aspects of S-phase checkpoint⁵⁴. Curiously, the signaling cascade that leads to Rad53 phosphorylation remains active, but origin firing becomes resistant to the suppressive checkpoint signals. Moreover, the sensitivity of *Stn1C* overproducing cells to HU appears to require *Stn1*-Pol12 interaction. Our observation that *Stn1C* can stimulate priming and the primase-to-polymerase transition suggests that these steps may be under S-phase checkpoint control, and that mis-regulation of these steps by pathologic concentrations of *Stn1C* may overcome checkpoint inhibition of DNA replication.

METHODS

Strains and plasmids

The *C. glabrata* strain *BG14* (*ura3::Tn903 G418^R*, a gift from Brendan Cormack, Johns Hopkins University) was used for the introduction of the tagged *PRI2* gene⁵⁵. For construction of FLAG₃-tagged *PRI2*, the full *PRI2* ORF with ~500 bp of 5' and 3' flanking sequences was amplified by PCR and inserted between the XhoI and XbaI site of the pGRB2.0 plasmid. The 3' end of the *PRI2* ORF was modified by Quikchange mutagenesis, resulting in the introduction of consecutive AvrII and BspEI restriction sites. A double stranded oligo carrying the FLAG₃ tag was then inserted between the two sites to yield pGRB2.0-PRI2-FG. The plasmid was transformed into *BG14*, and the resulting strain used for primase-Pol α purification.

Purification of Pol α, CST, Cdc13, Stn1 and truncation variants

The primase-Pol α (PP) complex was purified from *C. glabrata* as follows: The BG14 strain carrying pGRB2.0-PRI2-FG was grown in selective medium overnight until saturation. A suitable volume of saturated culture was used to inoculate 3-L YPD such that the initial OD₆₀₀ was ~ 0.5. The culture was grown to an OD₆₀₀ of 2.5, harvested, and re-suspend in Buffer TMG (10 mM Tris.HCl, pH 8.0, 1.2 mM MgCl₂, 0.1 mM EDTA, 0.1 mM EGTA, 200 mM Na-acetate, 10 % glycerol) at a ratio of 1 ml buffer per g wet weight. The cells were lysed by vortexing the suspension with an equal volume of glassbeads for a total of ~20 m (2 m pulses interspersed with 3 m cooling in ice-water bath). S100 supernatant was prepared by centrifuging the lysate in T-875 rotor (Sorvall) at 32,000 r.p.m. for 1 h. Extracts were subjected to M2 affinity purification as follows. The extracts were adjusted to the 2.5 mM MgCl₂, 1 mM DTT, 0.1% NP-40 and incubated with 1/80 vol of M2-Agarose resin at 4 °C on a rotator for 4 h. The resin was then washed 5 times with the FLAG binding buffer (1/8 vol of starting extract each time), and eluted with FLAG binding buffer containing 0.2 mg ml⁻¹ FLAG₃ peptide. For some assays, the M2-purified PP complex was further purified on a 5-ml 15–30% glycerol gradient in buffer G (50 mM Tris.HCl, pH 7.5, 150 mM NaCl, 2 mM DTT, 0.1% Triton X-100). The gradient was centrifuged at 42,000 rpm for 15 hours using a Sorvall AH-650 rotor. Twenty-five fractions were collected and assayed for polymerase activity and Pri2-FLAG₃ levels. The human PP complex was prepared by mixing equal molar concentrations of purified PRI1-PRI2 (from *E. coli*) and purified POL1-POL12 complex (from insect cells) as previously described⁵⁶.

The CST complex was purified from *E. coli* that carries expression plasmids for all three subunits as previously described⁴¹. Cdc13, Stn1, Stn1N, Stn1C, WH1, WH2 and human STN1 were each purified as His₆-SUMO-FLAG fusion proteins by sequential affinity chromatography as follows. The relevant ORFs with a C-terminal FLAG tag were generated by PCR and cloned downstream of the T7 promoter and the His₆-SUMO tag in the pSMT3 vector. The expression plasmid was introduced into the BL21(DE3) codon plus strain and the proteins purified through Ni-NTA and M2 agarose. Ten1 was purified as a GST fusion protein using the pGEX-6P1 vector (GE Healthcare Inc.), the BL21(DE3) codon plus strain, and glutathione-Sepharose as previously described⁴¹. The concentrations of the proteins were all estimated by comparing their Coomassie staining intensities to a standard curve of

specified quantities of BSA. In the case of PP, the concentration was calculated based on the staining intensity of the Pol1 subunit.

Primase-Pol α activity assays and product analysis

Unless otherwise indicated, the coupled primase-polymerase assays were performed in 20 μ l volume containing 40 mM Tris.HCl, pH 7.6, 30 mM potassium acetate, 13 mM Mg acetate, 5 mM dithiothreitol, 0.05 mM EDTA, 5% glycerol, 0.1 mg ml⁻¹ bovine serum albumin, ~1–2 nM Pol α , ~40–120 nM CST (or CST subunits), 3 mM ATP, 0.5 mM CTP, 0.7 mM GTP, 1.7 mM UTP, 16 μ M dATP, 14 μ M dCTP, 12 μ M dGTP, 30 μ M dTTP, and various labeled nucleotides or deoxynucleotides. In the standard coupled primase-polymerase assay, P³²-dATP (5 μ Ci nmole⁻¹) was included. The concentration of poly-dT template DNA (~300 nt, Midland Certified Reagent Company Inc.) was 300 nM, and that of the CgG4 (64 nt) and HsG9 (54 nt) template 1 μ M. In some Poly-dT assays, only ATP and dATP were included. After incubation at 32°C for 60–90 m, reactions were treated with 100 μ l STOP solution (20 mM Tris.HCl, pH 8.0, 20 mM EDTA) and 100 μ l proteinase K solution (10 mM Tris.HCl, pH 8.0, 0.5% SDS, 0.15 mg ml⁻¹ proteinase K), and incubated at the same temperature for 30 m. For the primase-to-polymerase switch assays that detect simultaneously RNA and RNA-DNA oligomers, we replaced P³²-dATP with 16 μ M cold dATP, and cold ATP with P³²-ATP. The specific activities of P³²-ATP used are indicated in the relevant figure legends. The primase capping assays were identical to the switch assay except that cold dATP was replaced by ddATP.

For the “primase only” assays, labeled ATP was used as the sole nucleotide substrate. For the Klenow-based primase assays, the primase reaction was performed with or without CST using 3 mM unlabeled ATP as the only nucleotide. The DNA template/RNA primer products were then recovered and subjected to Klenow extension in the presence of labeled dATP².

To test just the DNA polymerase activity, we used poly-dT/rA₁₀ (150 nM poly-dT and 450 nM rA₁₀) as the pre-primed substrate and labeled dATP as the sole nucleotide. For an alternative DNA polymerase assay, the priming reaction was performed in the absence of CST using 3 mM unlabeled ATP as the only nucleotide. Upon completion of the primase reaction, the mixture was adjusted to 50 μ l containing 25 mM EDTA, 0.25 % SDS, and 0.2 mg ml⁻¹ proteinase K. After 30 m incubation at 32°C, the mixture was extracted once with phenol/chloroform/isoamyl alcohol, and then passed through a Centri-Spin 20 column (Princeton Separations Inc.) to remove free ATP. The template and oligo-rA primer were then recovered by ethanol precipitation and used as substrates for PP and CST in assays that use labeled dATP as the sole nucleotide.

To remove the RNA portions of the RNA-DNA chimeras, the products were incubated in 100 μ l of 0.3% SDS, 20 mM EDTA at 55°C for 10 m, followed by the addition of 15 μ l 2.5 M NaOH, and a further 2 h incubation at 55°C. The mixture was then neutralized by adding 25 μ l 2M acetic acid, and the DNA recovered by ethanol precipitation⁵⁷. For DNase I treatment, the reaction products from the coupled assays were incubated with 1 U DNase I at 37°C for 2h followed by ethanol precipitation. Pilot experiments indicate that longer incubation or additional DNase I did not result in further degradation of the chimera.

For electrophoretic analysis, the products from the various assays were recovered by ethanol precipitation in the presence of 2.5 M ammonium acetate, 15 $\mu\text{g ml}^{-1}$ glycogen and 15 $\mu\text{g ml}^{-1}$ tRNA. The samples were dissolved in 90% formamide, 20 mM EDTA, 1 mg ml^{-1} xylene cyanol, and 1 mg/ml bromophenol blue, boiled for 5 min, and then applied to a denaturing polyacrylamide gel. Three different gel recipes were used depending on the nature of the experiments. For standard poly-dT assays, products were analyzed in 13% acrylamide/7M urea/1X TBE gels. For assays designed to characterize short RNA oligomers, products were analyzed in 18% acrylamide/7M urea/1X TBE gels⁸. For assays with G-tail templates, products were analyzed in 10% acrylamide/7M urea/36% formamide/1X TBE gels. The high formamide concentration was needed to fully denature the extremely GC-rich template/product duplexes.

Analysis of Stn1-Pol12 interaction

The co-expression/pull down assays were performed as follows⁵⁸. The DNAs encoding the various Stn1 and Pol12 fragments (see Table S2 for the amino acids included in each expression construct) were amplified by PCR and cloned into the pSMT3 vector⁵⁹ and the pGEX6P-1 vector (GE Healthcare) to enable their expression as HIS₆-SUMO and GST-FLAG fusion proteins, respectively. Each HIS₆-SUMO fusion protein was expressed alone or co-expressed with a GST-FLAG fusion protein in *E. coli* BL21 (DE3). The growth and induction protocols as well as the extract preparation procedures were as previously described⁶⁰. For Anti-FLAG pull down assays, ~500 μl of 10 mg ml^{-1} extract was incubated with 20 μl of M2-agarose beads (Sigma) in the FLAG(250) buffer (50 mM Tris.HCl, pH 7.5, 250 mM NaCl, 10 % glycerol, 0.1 % NP-40, 2.5 mM MgCl₂, 1 mM DTT). Following incubation with constant mixing on a rotator at 4°C for 2 h, the beads were washed 5 times with 0.5 ml of the FLAG(150) buffer (same as FLAG(250) except that it contains 150 mM NaCl), and then the M2-bound proteins eluted with 60 μl FLAG(150) containing 0.2 mg ml^{-1} 3XFLAG peptide. The eluates were analyzed by SDS-polyacrylamide gel electrophoresis, followed by staining with Coomassie Brilliant Blue R-250 or Western blotting. The GST pull down assays were carried out using glutathione-Sepharose (GE Healthcare). The binding and washing buffers were identical to those of the M2 pull down assays, and the elution buffer consists of FLAG(150) supplemented with 15 mM reduced glutathione.

Supplementary Material

Refer to Web version on PubMed Central for supplementary material.

Acknowledgments

We are grateful to Brendan Cormack for providing *C. glabrata* strains and plasmids. We thank Weihang Chai for human STN1 cDNA. N.F.L. thanks members of his lab for comments on the manuscript. This research was supported by NSF MCB-1157305 and NIH GM107287 to N.F.L, and NIH T32 CA124334 and AG01228 to W.E.W.

REFERENCES

1. Johansson E, Macneill SA. The eukaryotic replicative DNA polymerases take shape. Trends Biochem Sci. 2010; 35:339–347. [PubMed: 20163964]

2. Kaguni LS, Rossignol JM, Conaway RC, Lehman IR. Isolation of an intact DNA polymerase-primase from embryos of *Drosophila melanogaster*. *Proc Natl Acad Sci U S A*. 1983; 80:2221–2225. [PubMed: 6403945]
3. Kaguni LS, Rossignol JM, Conaway RC, Banks GR, Lehman IR. Association of DNA primase with the beta/gamma subunits of DNA polymerase alpha from *Drosophila melanogaster* embryos. *J Biol Chem*. 1983; 258:9037–9039. [PubMed: 6409898]
4. Uchiyama M, Wang TS. The B-subunit of DNA polymerase alpha-primase associates with the origin recognition complex for initiation of DNA replication. *Mol Cell Biol*. 2004; 24:7419–7434. [PubMed: 15314153]
5. Zhou B, et al. Structural basis for the interaction of a hexameric replicative helicase with the regulatory subunit of human DNA polymerase alpha-primase. *J Biol Chem*. 2012; 287:26854–26866. [PubMed: 22700977]
6. Klinge S, Hirst J, Maman JD, Krude T, Pellegrini L. An iron-sulfur domain of the eukaryotic primase is essential for RNA primer synthesis. *Nat Struct Mol Biol*. 2007; 14:875–877. [PubMed: 17704817]
7. Kilkenny ML, Longo MA, Perera RL, Pellegrini L. Structures of human primase reveal design of nucleotide elongation site and mode of Pol alpha tethering. *Proc Natl Acad Sci U S A*. 2013; 110:15961–15966. [PubMed: 24043831]
8. Kuchta RD, Reid B, Chang LM. DNA primase. Processivity and the primase to polymerase alpha activity switch. *J Biol Chem*. 1990; 265:16158–16165. [PubMed: 2398049]
9. Sheaff RJ, Kuchta RD, Iisley D. Calf thymus DNA polymerase alpha-primase: "communication" and primer-template movement between the two active sites. *Biochemistry*. 1994; 33:2247–2254. [PubMed: 8117681]
10. Nick McElhinny SA, Gordenin DA, Stith CM, Burgers PM, Kunkel TA. Division of labor at the eukaryotic replication fork. *Mol Cell*. 2008; 30:137–144. [PubMed: 18439893]
11. Jain D, Cooper JP. Telomeric strategies: means to an end. *Annu Rev Genet*. 2011; 44:243–269. [PubMed: 21047259]
12. de Lange T. How telomeres solve the end-protection problem. *Science*. 2009; 326:948–952. [PubMed: 19965504]
13. O'Sullivan RJ, Karlseder J. Telomeres: protecting chromosomes against genome instability. *Nat Rev Mol Cell Biol*. 2010; 11:171–181. [PubMed: 20125188]
14. Olovnikov A. A theory of marginotomy. The incomplete copying of template margin in enzymic synthesis of polynucleotides and biological significance of the phenomenon. *J Theor Biol*. 1973; 41:p181–p190.
15. Lue NF, Hsu M. A web of interactions at the ends. *Mol Cell*. 2011; 42:269–271. [PubMed: 21549304]
16. Blackburn EH, Collins K. Telomerase: an RNP enzyme synthesizes DNA. *Cold Spring Harb Perspect Biol*. 2011; 3
17. Nandakumar J, Cech TR. Finding the end: recruitment of telomerase to telomeres. *Nat Rev Mol Cell Biol*. 2013; 14:69–82. [PubMed: 23299958]
18. Adams Martin A, Dionne I, Wellinger RJ, Holm C. The function of DNA polymerase alpha at telomeric G tails is important for telomere homeostasis. *Mol Cell Biol*. 2000; 20:p786–p796.
19. Qi H, Zakian VA. The *Saccharomyces* telomere-binding protein Cdc13p interacts with both the catalytic subunit of DNA polymerase alpha and the telomerase-associated est1 protein. *Genes Dev*. 2000; 14:p1777–p1788.
20. Reveal PM, Henkels KM, Turchi JJ. Synthesis of the mammalian telomere lagging strand in vitro. *J Biol Chem*. 1997; 272:11678–11681. [PubMed: 9115215]
21. Giraud-Panis MJ, Teixeira MT, Geli V, Gilson E. CST meets shelterin to keep telomeres in check. *Mol Cell*. 2010; 39:665–676. [PubMed: 20832719]
22. Chen LY, Lingner J. CST for the grand finale of telomere replication. *Nucleus*. 2013; 4:277–282. [PubMed: 23851344]
23. Price CM, et al. Evolution of CST function in telomere maintenance. *Cell Cycle*. 2010; 9:3157–3165. [PubMed: 20697207]

24. Maringele L, Lydall D. EXO1-dependent single-stranded DNA at telomeres activates subsets of DNA damage and spindle checkpoint pathways in budding yeast yku70Delta mutants. *Genes Dev.* 2002; 16:p1919–p1933.
25. Dewar JM, Lydall D. Pif1- and Exo1-dependent nucleases coordinate checkpoint activation following telomere uncapping. *EMBO J.* 2010; 29:4020–4034. [PubMed: 21045806]
26. Miyake Y, et al. RPA-like mammalian Ctc1-Stn1-Ten1 complex binds to single-stranded DNA and protects telomeres independently of the Pot1 pathway. *Mol Cell.* 2009; 36:193–206. [PubMed: 19854130]
27. Surovtseva YV, et al. Conserved telomere maintenance component 1 interacts with STN1 and maintains chromosome ends in higher eukaryotes. *Mol Cell.* 2009; 36:207–218. [PubMed: 19854131]
28. Casteel DE, et al. A DNA polymerase- α primase cofactor with homology to replication protein A-32 regulates DNA replication in mammalian cells. *J Biol Chem.* 2009; 284:5807–5818. [PubMed: 19119139]
29. Goulian M, Heard CJ, Grimm SL. Purification and properties of an accessory protein for DNA polymerase alpha/primase. *J Biol Chem.* 1990; 265:13221–13230. [PubMed: 2165497]
30. Goulian M, Heard CJ. The mechanism of action of an accessory protein for DNA polymerase alpha/primase. *J Biol Chem.* 1990; 265:13231–13239. [PubMed: 2376593]
31. Huang C, Dai X, Chai W. Human Stn1 protects telomere integrity by promoting efficient lagging-strand synthesis at telomeres and mediating C-strand fill-in. *Cell Res.* 2012; 22:1681–1695. [PubMed: 22964711]
32. Stewart JA, et al. Human CST promotes telomere duplex replication and general replication restart after fork stalling. *EMBO J.* 2012; 31:3537–3549. [PubMed: 22863775]
33. Gu P, et al. CTC1 deletion results in defective telomere replication, leading to catastrophic telomere loss and stem cell exhaustion. *EMBO J.* 2012; 31:2309–2321. [PubMed: 22531781]
34. Kasbek C, Wang F, Price CM. Human TEN1 Maintains Telomere Integrity and Functions in Genome-wide Replication Restart. *J Biol Chem.* 2013; 288:30139–30150. [PubMed: 24025336]
35. Wang F, et al. Human CST has independent functions during telomere duplex replication and C-strand fill-in. *Cell Rep.* 2012; 2:1096–1103. [PubMed: 23142664]
36. Gelinas AD, et al. Telomere capping proteins are structurally related to RPA with an additional telomere-specific domain. *Proc Natl Acad Sci U S A.* 2009; 106:19298–19303. [PubMed: 19884503]
37. Sun J, et al. Stn1-Ten1 is an Rpa2-Rpa3-like complex at telomeres. *Genes Dev.* 2009; 23:2900–2914. [PubMed: 20008938]
38. Wold MS. Replication protein A: a heterotrimeric, single-stranded DNA-binding protein required for eukaryotic DNA metabolism. *Annu Rev Biochem.* 1997; 66:61–92. [PubMed: 9242902]
39. Gao H, Cervantes RB, Mandell EK, Otero JH, Lundblad V. RPA-like proteins mediate yeast telomere function. *Nat Struct Mol Biol.* 2007; 14:208–214. [PubMed: 17293872]
40. Nakaoka H, Nishiyama A, Saito M, Ishikawa F. *Xenopus laevis* Ctc1-Stn1-Ten1 (xST) protein complex is involved in priming DNA synthesis on single-stranded DNA template in *Xenopus* egg extract. *J Biol Chem.* 2011; 287:619–627. [PubMed: 22086929]
41. Lue NF, et al. The telomere capping complex CST has an unusual stoichiometry, makes multipartite interaction with G-Tails, and unfolds higher-order G-tail structures. *PLoS Genet.* 2013; 9:e1003145. [PubMed: 23300477]
42. Nick McElhinny SA, et al. Abundant ribonucleotide incorporation into DNA by yeast replicative polymerases. *Proc Natl Acad Sci U S A.* 2010; 107:4949–4954. [PubMed: 20194773]
43. Perera RL, et al. Mechanism for priming DNA synthesis by yeast DNA Polymerase alpha. *Elife.* 2013; 2:e00482. [PubMed: 23599895]
44. Nunez-Ramirez R, et al. Flexible tethering of primase and DNA Pol alpha in the eukaryotic primosome. *Nucleic Acids Res.* 2011; 39:8187–8199. [PubMed: 21715379]
45. Sun J, et al. Structural bases of dimerization of yeast telomere protein Cdc13 and its interaction with the catalytic subunit of DNA polymerase alpha. *Cell Res.* 2011; 21:258–274. [PubMed: 20877309]

46. Puglisi A, Bianchi A, Lemmens L, Damay P, Shore D. Distinct roles for yeast Stn1 in telomere capping and telomerase inhibition. *EMBO J.* 2008; 27:2328–2339. [PubMed: 19172739]
47. Klinge S, Nunez-Ramirez R, Llorca O, Pellegrini L. 3D architecture of DNA Pol alpha reveals the functional core of multi-subunit replicative polymerases. *EMBO J.* 2009; 28:1978–1987. [PubMed: 19494830]
48. Mer G, et al. Structural basis for the recognition of DNA repair proteins UNG2, XPA, and RAD52 by replication factor RPA. *Cell.* 2000; 103:449–456. [PubMed: 11081631]
49. Braun KA, Lao Y, He Z, Ingles CJ, Wold MS. Role of protein-protein interactions in the function of replication protein A (RPA): RPA modulates the activity of DNA polymerase alpha by multiple mechanisms. *Biochemistry.* 1997; 36:8443–8454. [PubMed: 9214288]
50. Song X, et al. STN1 protects chromosome ends in *Arabidopsis thaliana*. *Proc Natl Acad Sci U S A.* 2008; 105:19815–19820. [PubMed: 19064932]
51. D'Urso G, Grallert B, Nurse P. DNA polymerase alpha, a component of the replication initiation complex, is essential for the checkpoint coupling S phase to mitosis in fission yeast. *J Cell Sci.* 1995; 108(Pt 9):3109–3118. [PubMed: 8537450]
52. Byun TS, Pacek M, Yee MC, Walter JC, Cimprich KA. Functional uncoupling of MCM helicase and DNA polymerase activities activates the ATR-dependent checkpoint. *Genes Dev.* 2005; 19:1040–1052. [PubMed: 15833913]
53. Michael WM, Ott R, Fanning E, Newport J. Activation of the DNA replication checkpoint through RNA synthesis by primase. *Science.* 2000; 289:2133–2137. [PubMed: 11000117]
54. Gasparyan HJ, et al. Yeast telomere capping protein Stn1 overrides DNA replication control through the S phase checkpoint. *Proc Natl Acad Sci U S A.* 2009; 106:2206–2211. [PubMed: 19171895]
55. Cormack BP, Ghori N, Falkow S. An adhesin of the yeast pathogen *Candida glabrata* mediating adherence to human epithelial cells. *Science.* 1999; 285:578–582. [PubMed: 10417386]
56. Bermudez VP, Farina A, Tappin I, Hurwitz J. Influence of the human cohesion establishment factor Ctf4/AND-1 on DNA replication. *J Biol Chem.* 2010; 285:9493–9505. [PubMed: 20089864]
57. Sparks JL, et al. RNase H2-initiated ribonucleotide excision repair. *Mol Cell.* 2012; 47:980–986. [PubMed: 22864116]
58. Lue NF, Chan J. Duplication and functional specialization of the telomere-capping protein Cdc13 in *Candida* species. *J Biol Chem.* 2013; 288:29115–29123. [PubMed: 23965999]
59. Mossesso E, Lima CD. Ulp1-SUMO crystal structure and genetic analysis reveal conserved interactions and a regulatory element essential for cell growth in yeast. *Mol Cell.* 2000; 5:865–876. [PubMed: 10882122]
60. Yu EY, Sun J, Lei M, Lue NF. Analyses of *Candida* Cdc13 orthologues revealed a novel OB fold dimer arrangement, dimerization-assisted DNA binding, and substantial structural differences between Cdc13 and RPA70. *Mol Cell Biol.* 2012; 32:186–198. [PubMed: 22025677]

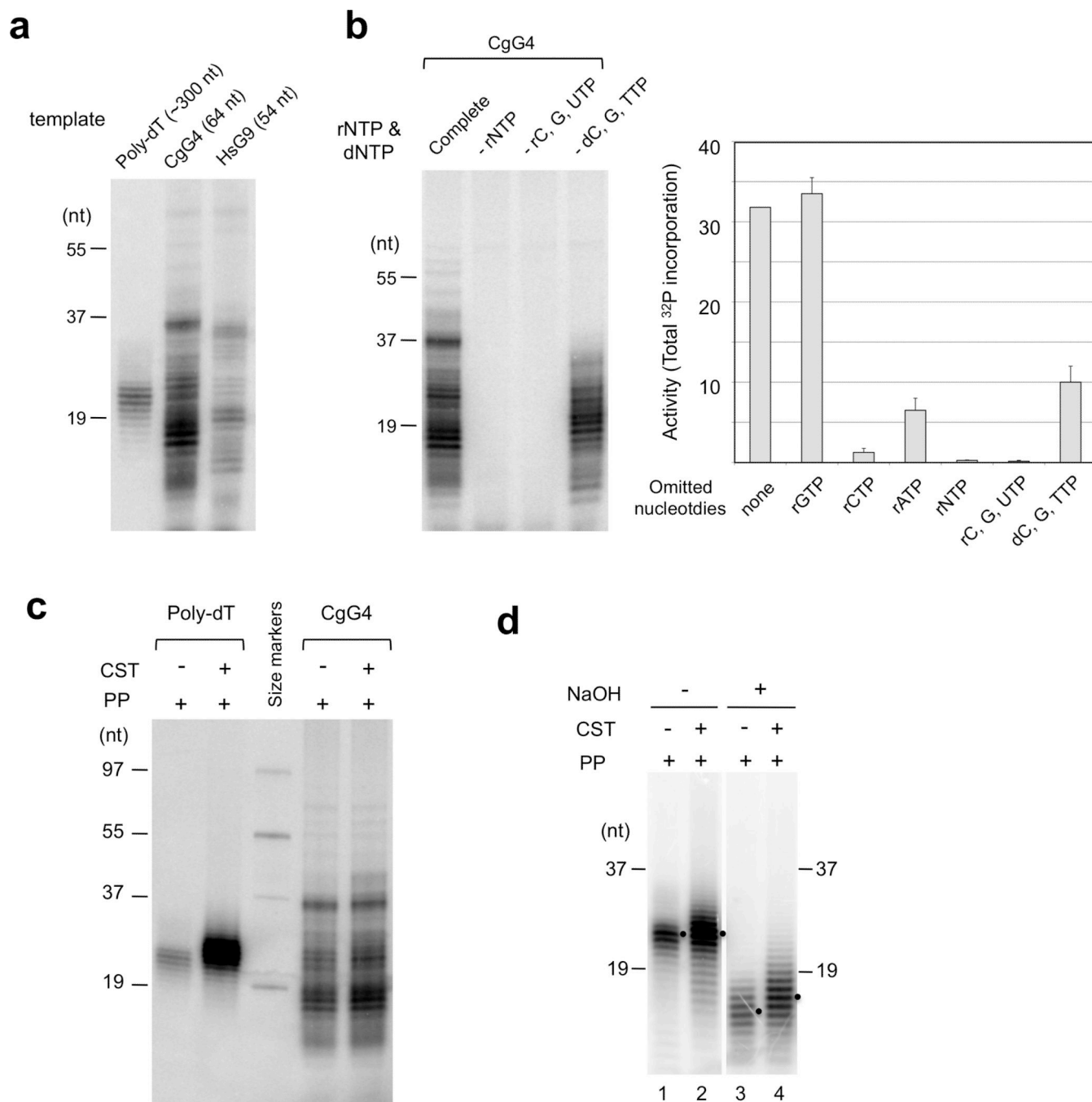


Figure 1. Characterization of the *C. glabrata* Pol α and the effect of CST on Pol α activity
(a) *C. glabrata* PP (2 nM) was subjected to coupled primase-polymerase assays using the indicated ssDNA templates (poly-dT, at 300 nM, CgG4 and HsG9 at 1 μ M). **(b)** PP (2 nM) was assayed using the CgG4 template and the indicated combinations of nucleotides. Total P^{32} incorporation into the products was quantified from PhosphorImager scans and plotted. Data (averages S.D.) are from three independent experiments. **(c)** The effect of CST (80 nM) on PP (1 nM) in the coupled primase-polymerase assays on poly-dT and CgG4 templates was analyzed. **(d)** The PP reaction products generated in the absence and presence of CST

were subjected to alkaline hydrolysis and analyzed in a 13 % acrylamide-TBE-urea gel. The peak product length for each sample is indicated by a black dot to the right.

Author Manuscript

Author Manuscript

Author Manuscript

Author Manuscript

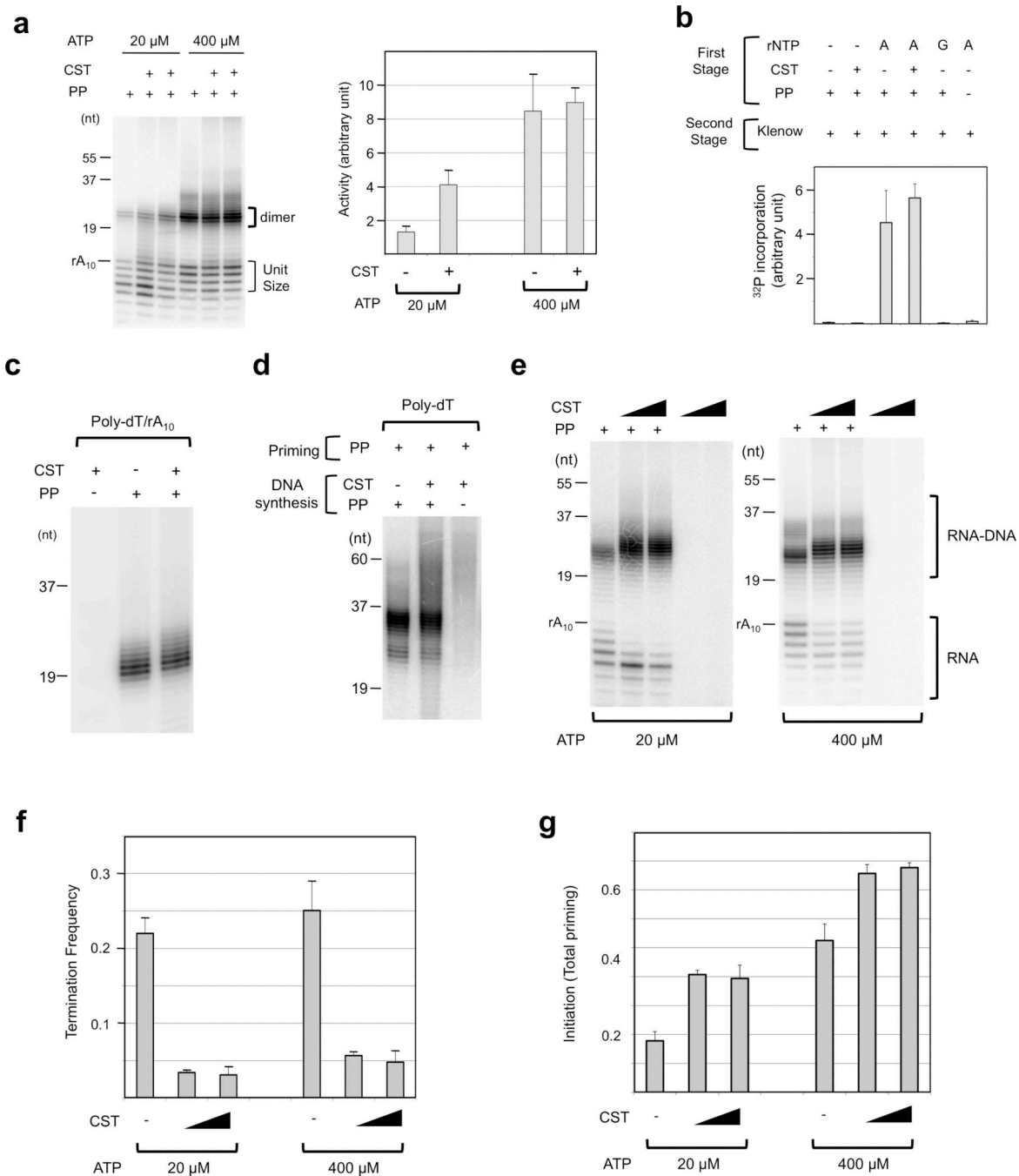


Figure 2. CST promotes RNA priming and the primase-to-polymerase transition

(a) The primase activity of the PP complex (1 nM) was analyzed at the indicated ATP concentrations in the absence or presence of CST (100 nM). Poly-dT was included at 300 nM, and P³²-ATP was included at 12 μ Ci nmole⁻¹ and 2.4 μ Ci nmole⁻¹ for the 20 μ M and 400 μ M ATP reactions, respectively. Size standards in this and several other assays include both ssDNA (19, 37, 55 and 97 nt) and ssRNA (rA₁₀). Results (averages S.D.) from three independent assays were quantified and plotted. (b) The two steps of the coupled “primase-Klenow” assay are illustrated on the left, and total ³²P incorporations plotted on the right. As

controls, the priming step of the reactions was performed using no ribonucleotides or GTP only. Data (averages S.D.) are from three independent sets of assays. **(c)** The DNA polymerase activity of PP (1 nM) was analyzed in the absence or presence of CST (100 nM) using as substrates “pre-primed” poly-dT/rA₁₀ (150 nM and 450 nM). **(d)** The DNA polymerase activity of PP (1 nM) was analyzed in the absence or presence of CST (150 nM) using as substrates the poly-dT/oligo-rA synthesized by PP in a priming reaction. **(e)** The primase-to-polymerase switch efficiency of PP (2 nM) was analyzed in the absence or presence of CST (100 and 200 nM) at the indicated ATP concentrations. P³²-ATP was included at 24 μCi nmole⁻¹ and 1.2 μCi nmole⁻¹ for the 20 μM and 400 μM ATP reactions, respectively. (Because the K_m of the primase for ribonucleotides is ~150 μM⁸, higher specific activity of P³²-ATP is needed to generate robust signals in the 20 μM ATP reactions). **(f)** The fractions of extendable RNA primers (i.e., 7–10 nt long) that were not lengthened by the polymerase into RNA-DNA chimeras in assays such as those shown in D were quantified and plotted. Data (averages S.D.) are from three independent sets of assays. **(g)** The total numbers of RNA and RNA-DNA products in assays such as those shown in D were calculated by summing the normalized intensities (normalized against the number of labeled rA in each product) and plotted. (For the RNA-DNA oligomer, we assume an average RNA length of 9.) Data (averages S.D.) are from three independent sets of assays.

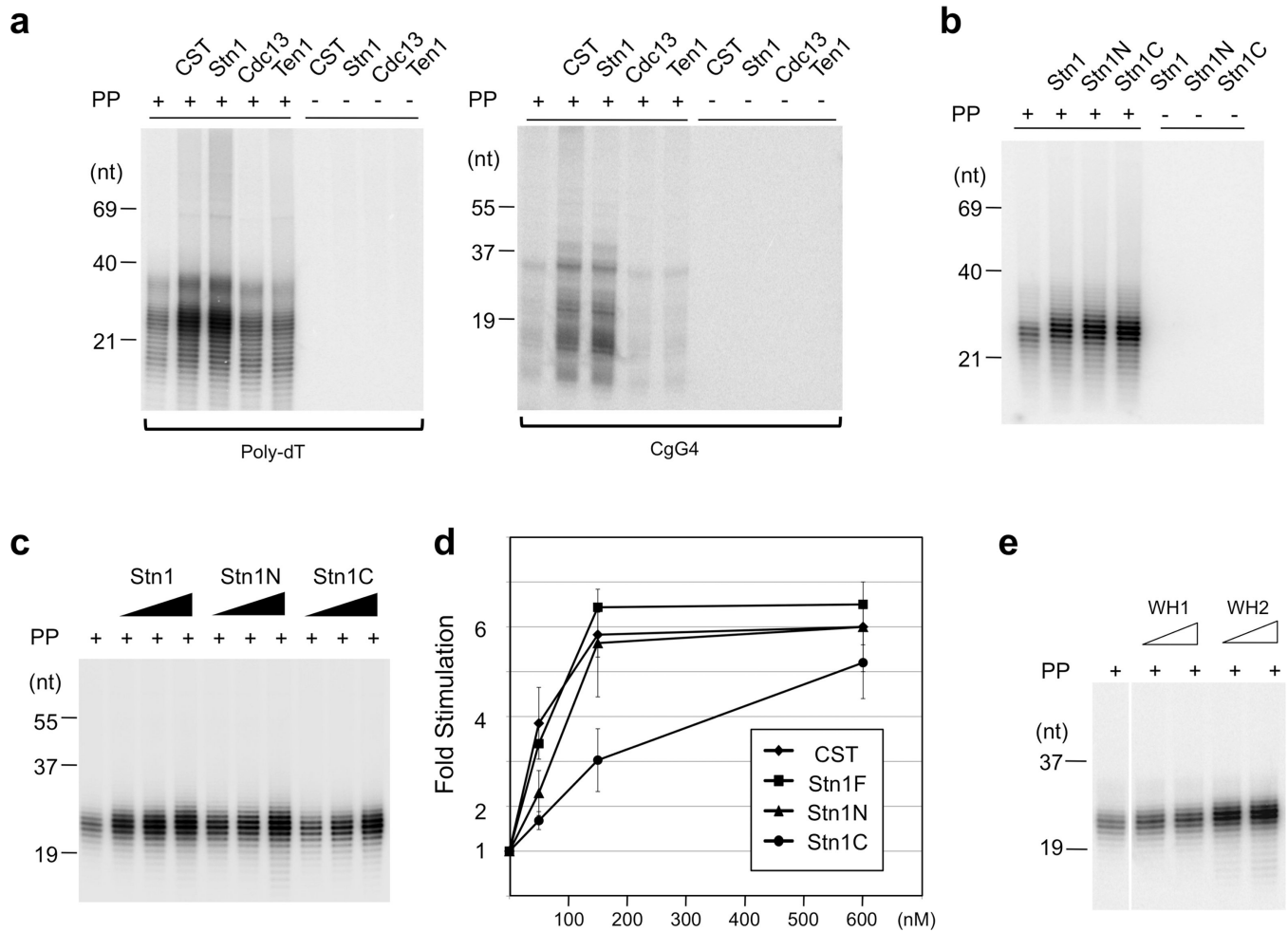


Figure 3. Stimulation of PP activity by CST, Stn1 and Stn1 variants

(a) (Left) The effects of CST complex and individual subunits (450 nM) on PP activity (2 nM) were analyzed in the coupled primase-polymerase assays using the poly-dT template. (Right) The effects of CST complex and individual subunits (450 nM) on PP activity (2 nM) were analyzed in the coupled primase-polymerase assays using the CgG4 template. (b) The effects of Full length Stn1 and the N- and C-terminus of Stn1 (1 μ M) on PP (2 nM) activity were analyzed in the coupled primase-polymerase assays using poly-dT template. (c) PP (1 nM) activity was assayed using poly-dT and varying concentrations (75, 150 and 600 nM) of Stn1, Stn1N, and Stn1C. (d) The stimulatory effects (averages S.D.) of varying concentrations of CST, Stn1, Stn1N and Stn1C from three independent experiments were quantified and plotted. (e) The stimulatory effects of WH1 and WH2 motifs of Stn1C (at 100 and 300 nM concentrations) were analyzed in the coupled primase-polymerase assays using the poly-dT template. The assays were from the same gel with several irrelevant lanes cropped out.

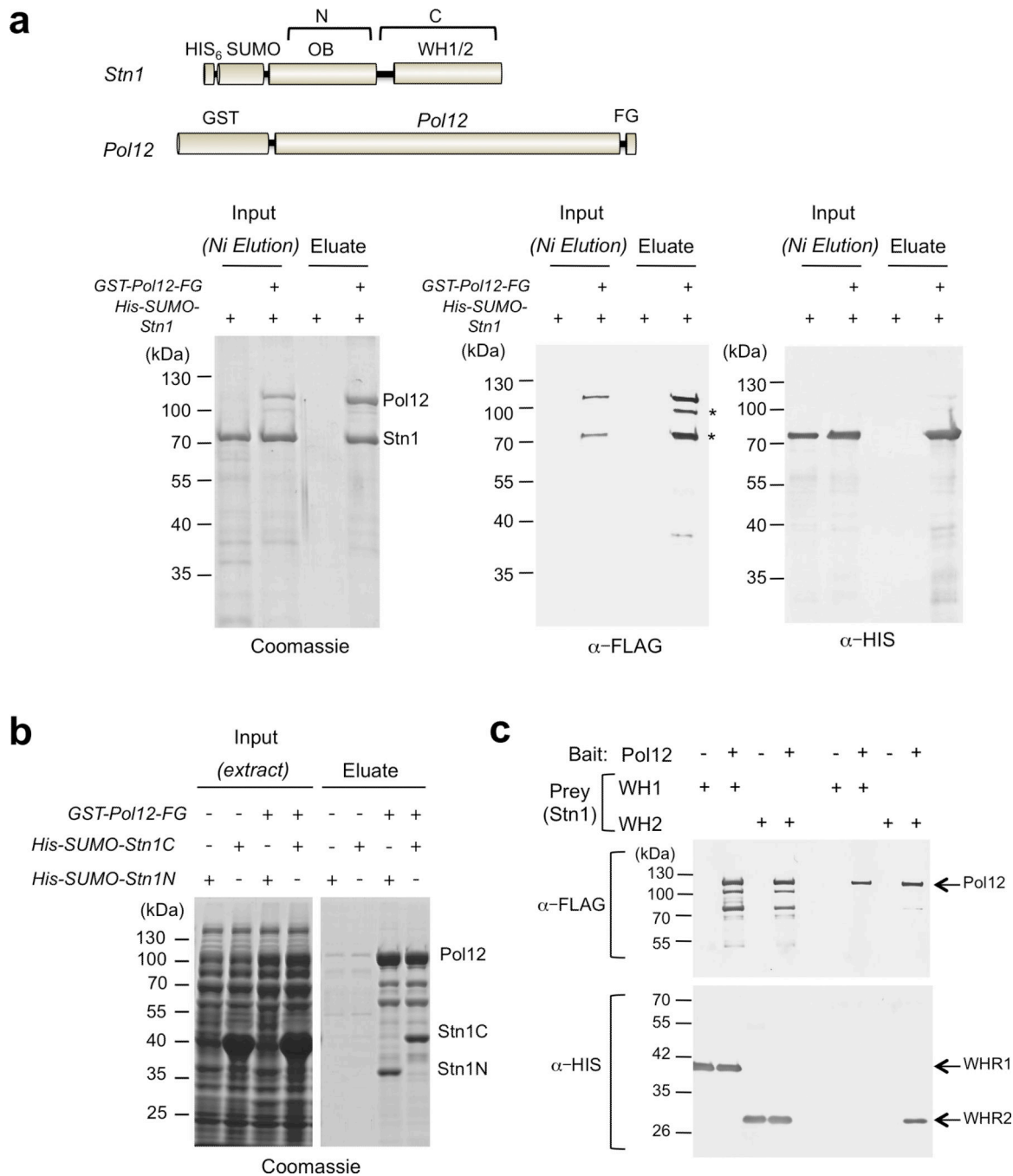


Figure 4. The physical interaction between Stn1 and Pol12

(a) A schematic depiction of the fusion tags used for the co-expression/pull down assays is shown at the top. Fractions derived from Ni-NTA purification of extracts containing Stn1 alone or Stn1 and Pol12 were subjected to anti-FLAG (M2) affinity purification. The input and purified fractions were subjected to SDS-PAGE, Coomassie staining, and Western analysis using the indicated antibodies. Two proteolytic fragments of Pol12 detected by anti-FLAG Western are indicated by asterisks. (b) Extracts from strains expressing Stn1 domains alone or in combination with Pol12 were subjected to M2 affinity purification, and the input

and purified fractions analyzed by SDS-PAGE and Coomassie staining. (c) Extracts from strains expressing Stn1C WH1 or WH2 motifs alone or in combination with Pol12 were subjected to GST affinity purification, and the input and purified fractions analyzed by Western. Pol12 was detected by anti-FLAG, whereas WH1 and WH2 anti-HIS antibodies.

Author Manuscript

Author Manuscript

Author Manuscript

Author Manuscript

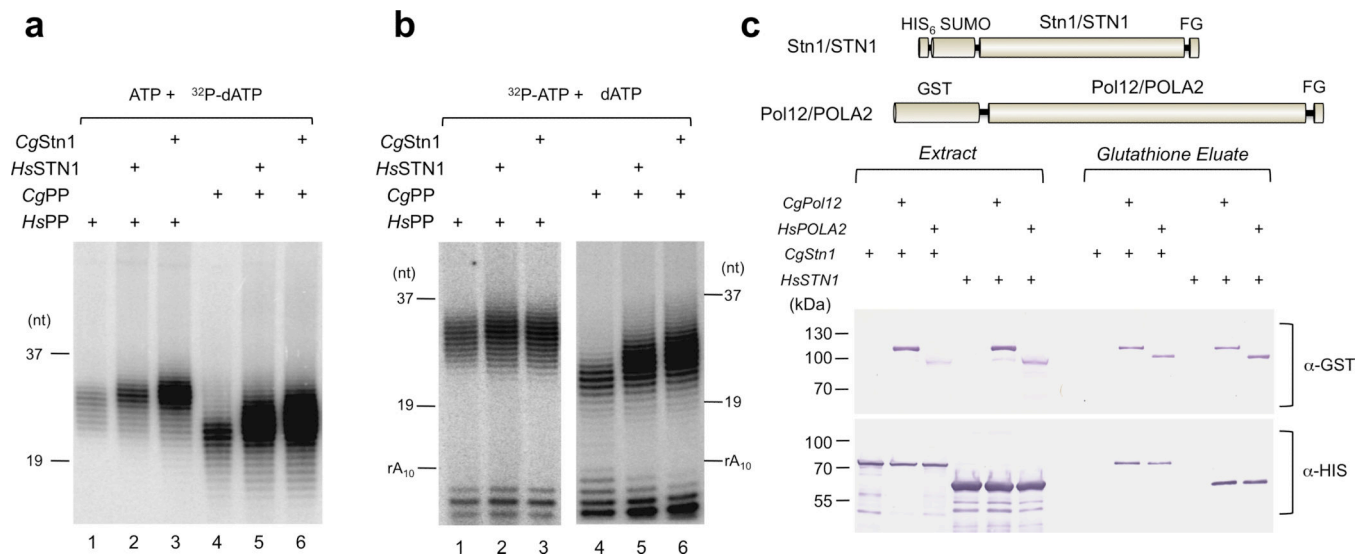


Figure 5. The intra-species and inter-species binding and stimulatory activities of *C. glabrata* and human Stn1

(a) *HsPP* and *CgPP* were analyzed in the absence or presence of *HsSTN1* or *CgStn1* using the poly-dT template, unlabeled ATP and labeled dATP. (b) *HsPP* and *CgPP* were analyzed in the absence or presence of *HsSTN1* or *CgStn1* using the poly-dT template, labeled ATP and unlabeled dATP.

(c) Extracts from strains expressing the indicated combinations of Pol12 and Stn1 were subjected to GST affinity purification, and the extracts and purified fractions analyzed by Western using anti-HIS and anti-GST antibodies.